Broadband stimulated four-wave parametric conversion on a tantalum pentoxide photonic chip

Ruiqi Y. Chen,[1,*] Martin D. B. Charlton,[1] and Pavlos G. Lagoudakis[2]

[1]*School of Electronics and Computer Science, University of Southampton, SO17 1BJ, UK*
[2]*School of Physics and Astronomy, University of Southampton, SO17 1BJ, UK*
*rc1@ecs.soton.ac.uk

Abstract: We exploit the large third order nonlinear susceptibility ($\chi^{(3)}$ or "Chi 3") of tantalum pentoxide (Ta_2O_5) planar waveguides and realize broadband optical parametric conversion on-chip. We use a co-linear pump-probe configuration and observe stimulated four wave parametric conversion when seeding either in the visible or the infrared. Pumping at 800 nm we observe parametric conversion over a broad spectral range with the parametric idler output spanning from 1200 nm to 1600 nm in infrared wavelengths and from 555 nm to 600 nm in visible wavelengths. Our demonstration of on-chip stimulated four wave parametric conversion introduces Ta_2O_5 as a novel material for broadband integrated nonlinear photonic circuit applications.

References and links

1. K. Okamoto, *Fundamentals of Optical Waveguides,* 2nd ed. (Academic Press, 2006), p. xvi, 561 pp.
2. R. W. Boyd, *Nonlinear Optics,* 3rd ed. (Academic, 2008), p. xix, 613 pp.
3. J. E. Sharping, M. Fiorentino, P. Kumar, and R. S. Windeler, "Optical parametric oscillator based on four-wave mixing in microstructure fiber," Opt. Lett. **27**(19), 1675–1677 (2002).
4. T. Sloanes, K. McEwan, B. Lowans, and L. Michaille, "Optimisation of high average power optical parametric generation using a photonic crystal fiber," Opt. Express **16**(24), 19724–19733 (2008).
5. M. A. Foster, A. C. Turner, J. E. Sharping, B. S. Schmidt, M. Lipson, and A. L. Gaeta, "Broad-band optical parametric gain on a silicon photonic chip," Nature **441**(7096), 960–963 (2006).
6. M. D. Pelusi, V. G. Ta'eed, M. R. E. Lamont, S. Madden, D. Y. Choi, B. Luther-Davies, and B. J. Eggleton, "Ultra-high nonlinear As_2S_3 planar waveguide for 160-Gb/s optical time-division demultiplexing by four-wave mixing," IEEE Photon. Technol. Lett. **19**(19), 1496–1498 (2007).
7. K. Yamada, H. Fukuda, T. Tsuchizawa, T. Watanabe, T. Shoji, and S. Itabashi, "All-optical efficient wavelength conversion using silicon photonic wire waveguide," IEEE Photon. Technol. Lett. **18**(9), 1046–1048 (2006).
8. M. D. Pelusi, V. G. Ta'eed, Libin Fu, E. Magi, M. R. E. Lamont, S. Madden, Duk-Yong Choi, D. A. P. Bulla, B. Luther-Davies, and B. J. Eggleton, "Applications of highly-nonlinear chalcogenide glass devices tailored for high-speed all-optical signal processing," IEEE J. Sel. Top. Quantum Electron. **14**(3), 529–539 (2008).
9. M. R. E. Lamont, B. Luther-Davies, D. Y. Choi, S. Madden, X. Gai, and B. J. Eggleton, "Net-gain from a parametric amplifier on a chalcogenide optical chip," Opt. Express **16**(25), 20374–20381 (2008).
10. F. Luan, M. D. Pelusi, M. R. E. Lamont, D. Y. Choi, S. Madden, B. Luther-Davies, and B. J. Eggleton, "Dispersion engineered As_2S_3 planar waveguides for broadband four-wave mixing based wavelength conversion of 40 Gb/s signals," Opt. Express **17**(5), 3514–3520 (2009).
11. M. D. Pelusi, F. Luan, S. Madden, D. Y. Choi, D. A. Bulla, B. Luther-Davies, and B. J. Eggleton, "Wavelength conversion of high-speed phase and intensity modulated signals using a highly nonlinear chalcogenide glass chip," IEEE Photon. Technol. Lett. **22**(1), 3–5 (2010).
12. J. Van Erps, F. Luan, M. D. Pelusi, T. Iredale, S. Madden, D. Y. Choi, D. A. Bulla, B. Luther-Davies, H. Thienpont, and B. J. Eggleton, "High-resolution optical sampling of 640-Gb/s data using four-wave mixing in dispersion-engineered highly nonlinear As_2S_3 planar waveguides," J. Lightwave Technol. **28**(2), 209–215 (2010).
13. I. W. Hsieh, X. Chen, J. I. Dadap, N. C. Panoiu, R. M. Osgood, S. J. McNab, and Y. A. Vlasov, "Ultrafast-pulse self-phase modulation and third-order dispersion in Si photonic wire-waveguides," Opt. Express **14**(25), 12380–12387 (2006).

14. J. I. Dadap, N. C. Panoiu, X. Chen, I. W. Hsieh, X. Liu, C.-Y. Chou, E. Dulkeith, S. J. McNab, F. Xia, W. M. J. Green, L. Sekaric, Y. A. Vlasov, and R. M. Osgood, Jr., "Nonlinear-optical phase modification in dispersion-engineered Si photonic wires," Opt. Express **16**(2), 1280–1299 (2008).
15. E. M. Dianov, I. A. Bufetov, A. A. Frolov, V. M. Mashinsky, V. G. Plotnichenko, M. F. Churbanov, and G. E. Snopatin, "Catastrophic destruction of fluoride and chalcogenide optical fibres," Electron. Lett. **38**(15), 783–784 (2002).
16. R. Stegeman, G. Stegeman, P. Delfyett, L. Petit, N. Carlie, K. Richardson, and M. Couzi, "Raman gain measurements and photo-induced transmission effects of germanium- and arsenic-based chalcogenide glasses," Opt. Express **14**(24), 11702–11708 (2006).
17. R. Y. Chen, M. D. B. Charlton, and P. G. Lagoudakis, "Reference free Chi 3 dispersion measurements in planar tantalum pentoxide waveguides," Proc. SPIE **7420**, 74200D (2009).
18. R. Y. Chen, M. D. B. Charlton, and P. G. Lagoudakis, "Chi 3 dispersion in planar tantalum pentoxide waveguides in the telecommunications window," Opt. Lett. **34**(7), 1135–1137 (2009).
19. R. Y. Chen, M. D. B. Charlton, and P. G. Lagoudakis, "Experimental demonstration of on-chip optical parametric oscillation in planar tantalum pentoxide waveguides," in *Optics Photonics 2010 (SPIE),* (San Diego, USA, 2010).
20. C. Chaneliere, J. L. Autran, R. A. B. Devine, and B. Balland, "Tantalum pentoxide (Ta_2O_5) thin films for advanced dielectric applications," Mater. Sci. Eng. Rep. **22**(6), 269–322 (1998).
21. J. D. Mills, T. Chaipiboonwong, W. S. Brocklesby, M. D. B. Charlton, M. E. Zoorob, C. Netti, and J. J. Baumberg, "Observation of the developing optical continuum along a nonlinear waveguide," Opt. Lett. **31**(16), 2459–2461 (2006).
22. W. Kaiser, *Ultrashort Laser Pulses and Applications*, Topics in applied physics (Springer, 1988), 424 pp.

1. Introduction

Stimulated optical four-wave parametric conversion, governed by degenerative four-wave mixing (DFWM), is an important $\chi^{(3)}$ nonlinear effect which can potentially provide a versatile tuneable solid state laser source capable of producing widely tuneable light sources in the infrared (IR), visible, and ultraviolet spectral regions, with either continuous-wave or pulsed optical pumping [1,2]. Stimulated optical four-wave parametric conversion has been reported widely in photonic crystal fibres [3,4], but there are only a few reports in planar waveguides [5,6]. Recent developments in optical communications and optical planar waveguides with core materials of silicon (Si) [5,7] and chalcogenide glass (As_2S_3) [6,8–12] show strong potential for utilizing this $\chi^{(3)}$ governed nonlinear process for broadband integrated nonlinear photonic circuit applications. Although Si demonstrates very high $\chi^{(3)}$ and refractive index, high intrinsic normal dispersion and free carrier creation losses are known issue with Si based devices [13,14]. Silicon also has the disadvantage of not being transparent in the visible wavelengths. Chalcogenide glass also has high normal dispersion and relatively low damage threshold of 9 GW/cm^2 [15,16]. Whereas low damage thresholds is a known issue for nonlinear photonic devices such as fibre lasers and chalcogenide glasses, the damage threshold for Ta_2O_5, exceeds peak power densities of 5×10^8 GW/m^2 . Ta_2O_5 also has the advantage that the fabrication process is well-known as it is commonly used as a high-k material in the microelectronics industry [17–20].

Here we demonstrate stimulated four-wave parametric conversion in the near infrared that spans over 400 nm, a four-fold improvement in operating bandwidth to previous broadband capabilities [5–12]. The majority of $\chi^{(3)}$ type parametric oscillators using fibres and waveguides are also seeded and pumped close to the telecommunication spectrum, where here we extend the operation to visible wavelengths.

We report broadband $\chi^{(3)}$ nonlinear optical four-wave parametric conversion tuneable over the wavelength range of 555 – 600 nm and 1200 – 1600 nm within a 7 mm long planar tantalum pentoxide (Ta_2O_5) waveguide using a co-linear pump-probe experimental setup. The waveguides demonstrate parametric conversion when seeded from either in the visible or near infrared wavelengths, in combination with a fixed pump at 800 nm. We measure the dispersion properties of the waveguides using a nonlinear time-of-flight (Kerr gate) arrangement, and compare the experimental results with finite element method (FEM)

simulation results obtained using RSoft CAD. The comparison shows that there is a possibility to make an integrated nonlinear photonic circuit based on four-wave parametric conversion using Ta_2O_5 planar waveguides.

2. Experiments

Ta_2O_5 waveguide samples were grown on a silicon substrate by radio frequency (RF) sputtering, optical lithography, and plasma etching [21]. Figure 1 shows a cross-sectional scanning electron microscope (SEM) image of the tested waveguide samples with thickness of 500 nm and widths of 6.6 μm, 9.41 μm, 9.85 μm, and 11.65 μm, designated from here on as guides G1, G2, G3, and G4, respectively. Robustness tests have previously shown that there is no change in waveguide loss or ultraviolet (UV) induced damage with up to 1 W of continuous wave (CW) 455 nm light focused into the guide, and no waveguide facet damage for 800 nm 250 fs pulses with energies up to 2 μJ at repetition rate of 250 kHz. Before commencing this investigation of nonlinear effects in the guides, further tests for laser induced damage were performed on a test guide. This showed that there was no induced waveguide damage for 150 fs pulses with 100 kHz repetition rate at: 800 nm, or output at wavelength range of 1200 – 1600 nm with energies up to 20 nJ /pulse, or 555 – 600 nm with energies up to 50 nJ /pulse.
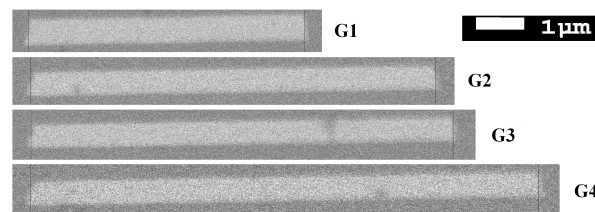

Fig. 1. Cross-sectional scanning electron microscope images of 7 mm long waveguide sample facets after damage test experiments. All waveguides have thickness of 500 and widths as follows: 6.6 µm (G1), 9.41 µm (G2), 9.85 µm (G3), and 11.65 µm (G4).
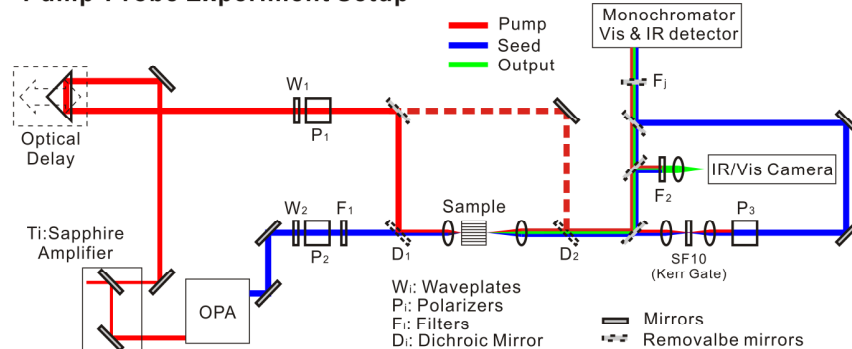

Fig. 2. Pump-probe experimental setup for demonstration of optical four-wave parametric conversion process.

Figure 2 shows the experimental setup used for the co-linear pump-probe experiment. The optical components used in this setup depend on the seed beam wavelength range. Anti-reflection coatings for waveplates (W$_i$), polarizers (P$_i$) and lenses are chosen to cover the seed beam wavelength range to avoid reflections. Central wavelength and type (long-pass/short-pass) of colour filters (F$_i$) all match the seed beam wavelength range to filter out the unwanted wavelengths from the pump. We observed the four wave parametric conversion process both

when seeding in the visible and in the infrared. Silicon dioxide (SiO_2) clad Ta_2O_5 planar rib waveguides were co-linearly excited with 800 nm pump beam and a visible/infrared seed beam. The visible seed beam was tuned over the wavelength range of 555 – 600 nm with average powers of 0.01 – 5.0 mW. The IR seed beam was tuned over the wavelength range of 1200 – 1600 nm with average powers of 0.01 – 2 mW. The range of average pump power was 1.0 – 13.0 mW. For all beams the power was measured before coupling to the sample.

3. Results

Figure 3a shows the parametric output intensity dependence on 800nm pump-power for guide G4, when seeded with 5 mW average power at 601 nm. As expected the parametric output intensity increases with increasing pump power. Figure 3b plots the integrated intensity of the output spectrum vs. pump power (dots). The solid line is a fit to the expected square power dependence, $I_{output} = A \cdot I_{pump}^2$, where the proportionality coefficient A relates to $\chi^{(3)}$ [18]. Figure 3c shows the output wavelength dependence on the seed wavelength satisfying energy conservation in the parametric process.
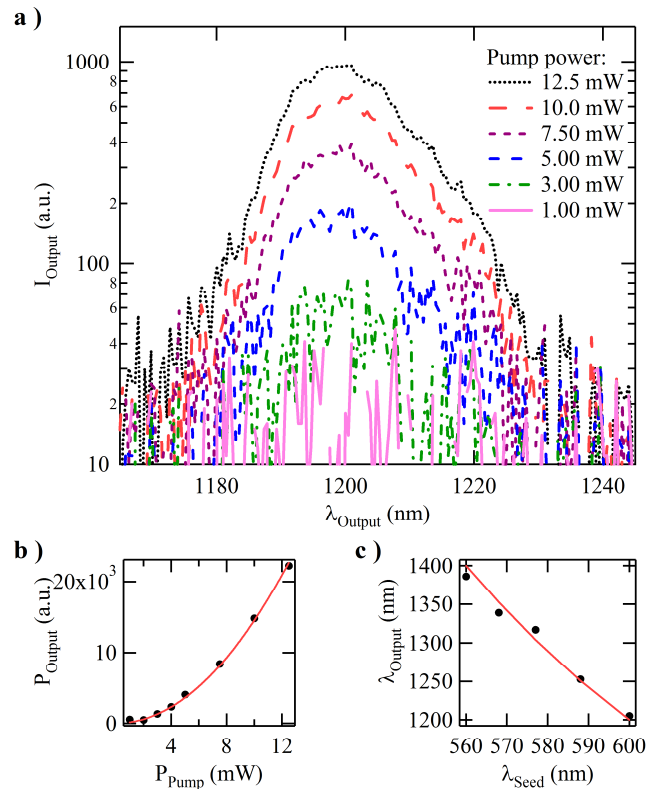

Fig. 3. a) Pump power dependence of parametric output for 601 nm seed; b) Spectrally integrated intensity of output vs. pump power (dots), the solid line is a fit to the pump squared dependence; c) Output wavelength dependence on seed wavelength (dots), the solid line plots the energy conservation imposed on the parametric process.

Figure 4a shows that for a fixed pump power, the output intensity also increases with increasing visible seed power. However, we observe saturation of the output intensity as a function of seed power. Figure 4b shows the saturation of the spectrally integrated output intensity with increasing seed power, which is attributed to conversion efficiency saturation.
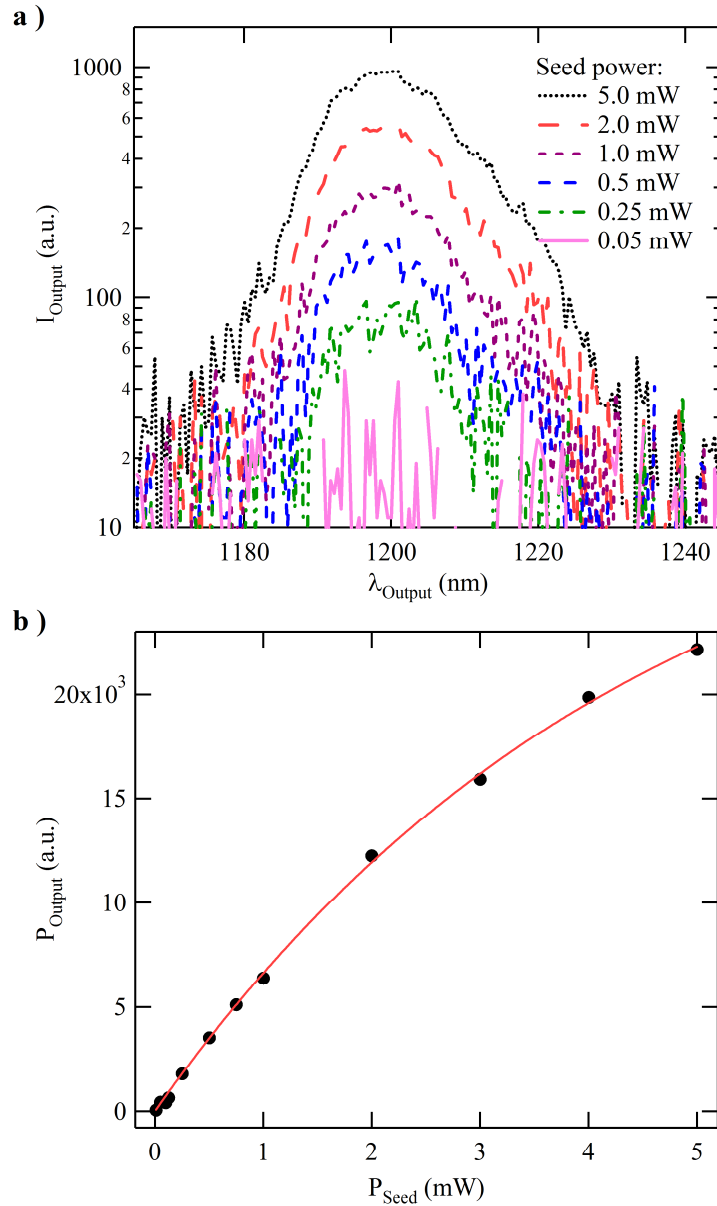
a)

b)

Fig. 4. a) Output seed power dependence for 601 nm seed and 800 nm pump at 12.5 mW; b) Spectrally integrated intensity of output vs. seed power (dots), the solid line is a guide to the eye.

The waveguide G2 used for visible seeding experiments was also pumped with co-linear coupled 800 nm pump and IR seed beams. The IR seed wavelength was tuned over the range 1200 – 1600 nm, in 50 nm steps. Although the average power for IR seed is below 2 mW for all selected wavelengths, it was sufficient to stimulate the $\chi^{(3)}$ parametric process. The pump power dependence measurements were taken over an average pump power range of 0.50 – 13.0 mW. The outputs show visible spectra with parametric outputs and third-harmonic output; note the third harmonic generation (THG) signal cannot be detected by the spectrometer below 480 nm.

Figure 5a shows pump (800 nm) power dependence of the output spectra from the pump-probe experiment for seeding at around 1550 nm at a fixed power of 2 mW. The constant output spectra intensity around 520 nm indicates that the THG output is not affected by the pump power, i.e. the third harmonic is generated only by the seed beam. The parametric output shows a peak at 540 nm as expected for the parametric conversion. The power dependence between 800nm pump and the visible output follows the expected quadratic relation as shown in Fig. 5b. Figure 5c shows the output profiles from the examined IR seed wavelengths including the THG signal. The figure also shows the corresponding parametric output peak wavelength.
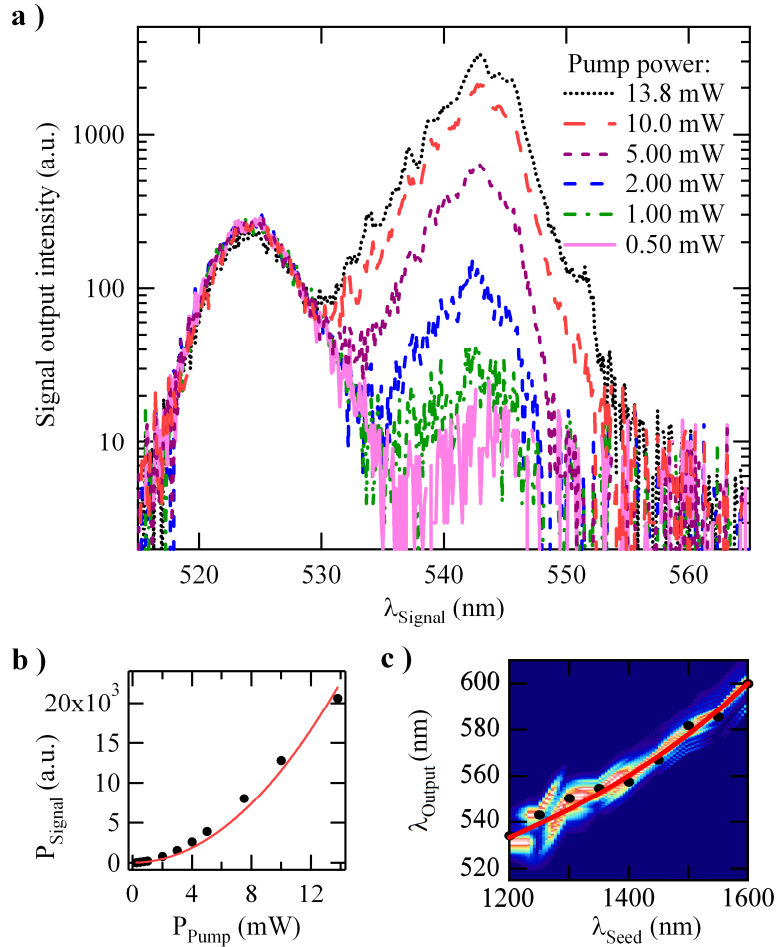

Fig. 5. a) Pump power dependence of output for 1550 nm seed; b) spectrally integrated intensity of output (excluding the THG) vs. pump power (dots), the solid line is fit to the pump squared dependence; c) output wavelength dependence on seed wavelength (dots), the solid line is the phase matching imposed on the parametric process. The background image shows spectral intensity of the output.

4. Theory and discussions

In what follows we discuss the efficiency of the process when seeded in the visible and IR as well as the dependence of the phase matching term on the temporal overlap of the seed and pump pulses. The broadband tuneable optical parametric process we investigate is a third-order nonlinear degenerative four-wave mixing process. The parametric process combines

two pump photons and one seed photon to generate one output photon as shown in Fig. 6. The relationship between the three photons can be expressed as [2]:

$$\omega_{output} = 2\omega_{pump} - \omega_{seed}$$

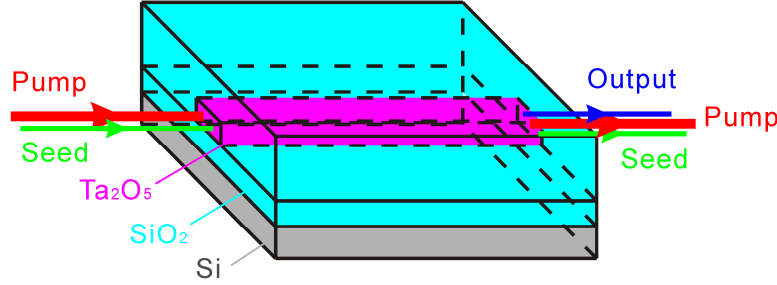where, $\omega_{output} \neq 2\omega_{pump} \neq \omega_{seed}$

Fig. 6. Illustrations of the co-linear parametric conversion process in planar waveguides.

The intensity dependence of the output (I_{output}) on the pump (I_{pump}) and seed intensity (I_{seed}) for the non-depleted pump regime is given by [22]:

$$I_{output} = C \cdot \left| \chi^{(3)} \right|^2 \cdot I_{pump}^2 \cdot I_{seed} \cdot l^2 \cdot \left[\frac{\sin(\Delta k \cdot l / 2)}{\Delta k \cdot l / 2} \right]^2$$

where $\Delta k = 2k_{pump} - k_{output} - k_{seed}$ is the wave number difference where the wave number $k = \frac{2\pi \cdot n_{eff}}{\lambda}$ for each component, and $C = \frac{\omega_{output}^2}{(cn_0)^4 \cdot \varepsilon_0^2}$.

The output intensity (I_{output}) versus the pump intensity (I_{pump}) follows a quadratic relationship, i.e. $I_{output} = A \cdot I_{pump}^2$, as shown both in the IR and visible seed experiments (Figs. 3b and 5b). Due to higher $\chi^{(3)}$ in the IR the nonlinear process is more efficient in the case of IR seeding as observed from a comparison of Figs. 3b and 5b.

The time-delay between pump and seed pulses shows the tunability of the process over the bandwidth of the input pulse. Figure 7 shows that the output spectrum is affected by the time-delay between the pump and visible (Figs. 7a, 7b, and 7c) or IR (Fig. 7d) seed beams. The output spectrum measured at each delay time tunes over a range of 100 fs either side of zero-time delay. It is therefore feasible to achieve narrow band continuous wavelength tuning by adjusting the time-delay between the pump and seed pulses over the available bandwidth of the seed beam.
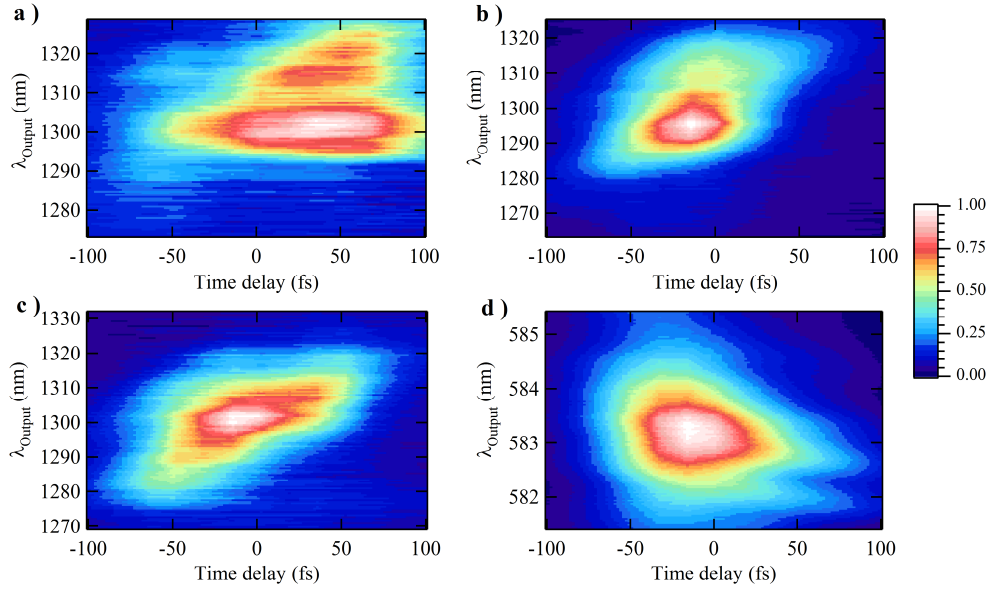
Fig. 7. Time dependent measured idler spectrum from tested waveguides (intensity in false colour) for both visible and IR seeds with time delay tuned over a range of 100 fs with respect to zero-time delay. a) guide G1 seeded at 577 nm; b) guide G3 seeded at 577 nm; c) guide G4 seeded at 577 nm; d) guide G2 seeded at 1300 nm.

The other factor that affects the phase-matching for FWM is the dispersion of the waveguides with respect to seed wavelength which is charactersied using time-of-flight (Kerr gate). White light supercontinuum generated in a sapphire plate is coupled into the waveguides and the output is characterised using a Kerr gate. The effective mode index of the supported modes for one particular wavelength is measured by tuning the time-delay between pump and white light pulses. For comparison the dispersion, (i.e. the effective mode index), of the waveguides is also obtained from simulations by Finite Element Method. We use RSoft CAD to simulate the waveguide dispersion of 12 supported modes, numbered as mode $0 - 11$, which incorporates the Ta_2O_5 material dispersion [17,18] in waveguide G2. Figure 8a shows the measured waveguide output mode images generated by the stimulated four-wave parametric process, and Fig. 8b shows the measured dispersion, superimposed with the simulated effective mode index of 12 supported modes in the examined waveguide (G2). The results of Fig. 8b show that waveguide output modes are supported continuously across the examined wavelength range, although there is some mode hopping. Given sufficient bandwidth of the input seed it is therefore possible to tune the FWM output wavelength continuously over this range by adjusting the phase-matching.
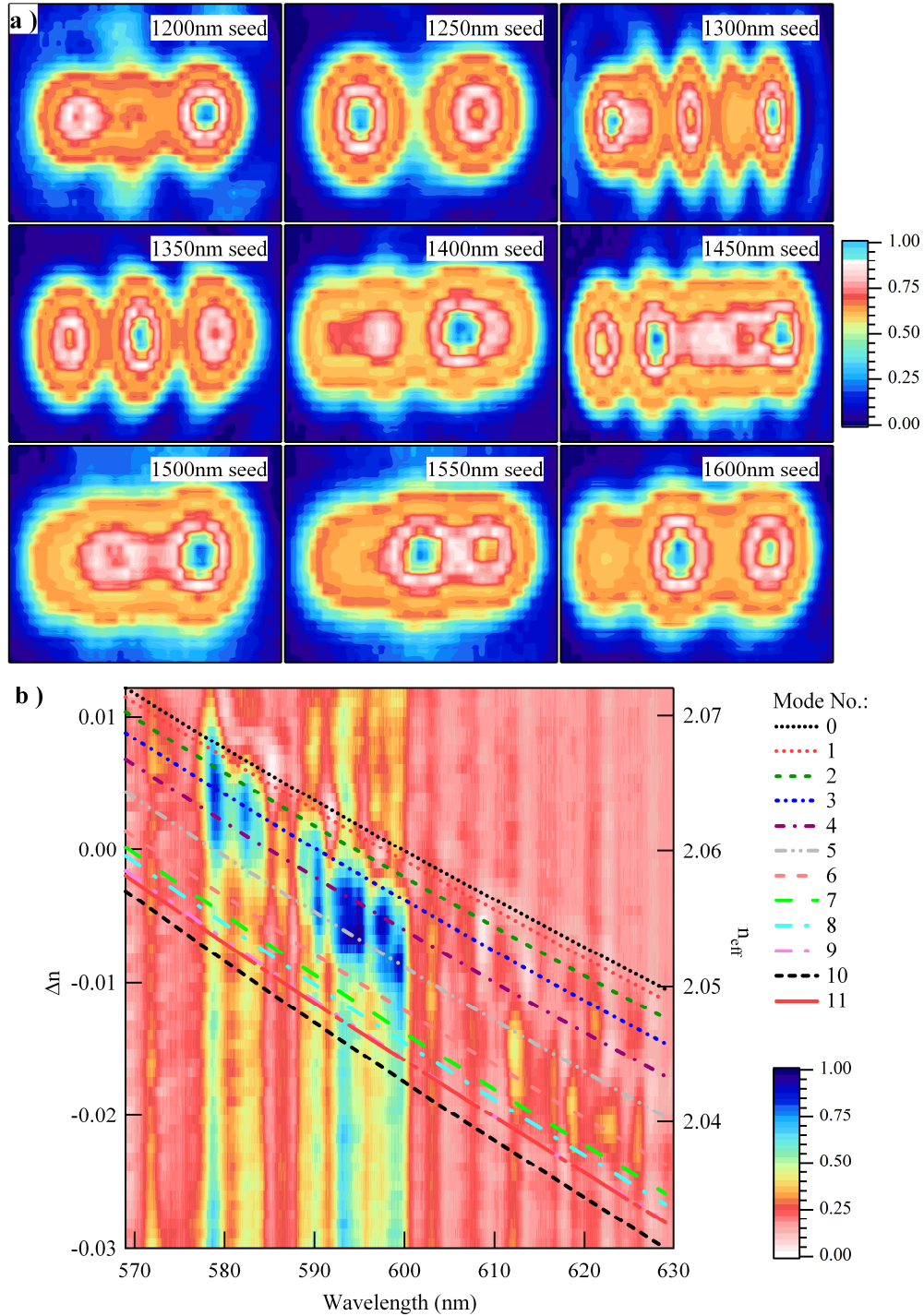
Fig. 8. a) output mode images from stimulated four-wave parametric process; b) dispersion measurements using a time-of-flight (Kerr gate) setup superimposed with the simulations of the refractive index for 12 supported modes in the examined waveguide (G2). The left hand axis relates to the colour map and shows change in measured effective mode index calculated from time-of-flight as a function of wavelength. The right hand axis relates to the lines, and displays calculated effective mode index as a function of wavelength.

5. Conclusions

In conclusion, we have observed widely tuneable optical parametric conversion in 7 mm long Ta_2O_5 planar rib waveguides. We have demonstrated that the parametric conversion is attainable both in the visible and near-infrared spectrum with a bandwidth of 45 nm and 400 nm respectively. We have also demonstrated phase dependent tuning of 40 nm in the IR (within the limits imposed by the bandwidth of a fixed wavelength input pulse). We also investigated the dispersion properties of the waveguides through Kerr gate time-of-flight measurements. Experimental evidence and theoretical analysis of the waveguide dispersion properties shows that this could be extended greatly given a suitable broad bandwidth seed. Our demonstration of on-chip stimulated four wave parametric conversion introduces Ta_2O_5 as a novel material for broadband integrated nonlinear photonic circuit applications.